CSCE Annual Conference

*Growing with youth – Croître avec les jeunes*

Laval (Greater Montreal)

June 12 - 15, 2019

# PUNCHING BEHAVIOR OF GFRP-RC EDGE FLAT PLATE CONNECTIONS REINFORCED WITH SHEAR REINFORCEMENT

Ahmed E. Salama[1], Mohamed Hassan[2], Brahim Benmokrane[3]
[1,3] Department of Civil Engineering, University of Sherbrooke, Sherbrooke, Quebec, Canada
[1]Ahmed.Salama@USherbrooke.ca
[2]Mohamed.Hassan@USherbrooke.ca
[3]Brahim.Benmokrane@USherbrooke.ca

**Abstract:** This paper presents an experimental investigation aimed at evaluating the effectiveness of glass-fiber-reinforced-polymer (GFRP) stirrups as shear reinforcement in GFRP edge slab–column connections. Three full-scale GFRP edge slab–column connections were tested under combined vertical shear force (V) and unbalanced moment (M) with (M/V) ratio equal 0.3. The slabs measured 2500×1350×200 mm with a 300 mm square column extending 700 mm above and below the slab surfaces. The edge connections were reinforced in shear with GFRP stirrups, closed or spiral, placed in orthogonal layout. Utilizing either closed or spiral stirrups as shear reinforcement around the punching shear zone showed substantial improvement on the slab behavior, whereas the mode of failure was changed from a brittle punching failure for slab without shear reinforcement to a softer punching failure for slab with shear reinforcement.

## 1 INTRODUCTION

Reinforced-concrete (RC) two-way flat-slab systems are very popular in construction because of their functional and economic advantages. Yet this type of structural system is not very efficient in terms of energy dissipation and is vulnerable to a type of brittle failure known as a punching-shear failure. When designing edge slab–column connections, the lack of symmetry of the portion of the slab resisting the punching action and relatively large unbalanced moments to be transferred between the slab and column may produce significant shear stresses that increase the likelihood of brittle failure, which must be considered. The avoidance of such a failure is of paramount importance. Various solutions have been used in the past to mitigate punching-shear failure at a slab–column connection. This can be achieved by simply (1) increasing the slab thickness by providing a drop panel or capital or increasing the column dimensions; (2) using higher-strength concrete; or (3) providing additional shear strength through shear reinforcement in the form of stirrups, shear studs, shear heads, or shear bands within the slab around the column perimeter. The latter solution is more effective and practical than the other two methods in increasing the punching-shear strength and deformation capacity of slab–column connections (Megally and Ghali 2000 and Lips et al. 2012), which is one of the primary motivations of this research.

Despite the increasing demand to use GFRP reinforcing bars in two-way flat slabs, (Ospina et al. 2003; Lee et al. 2009; Dulude et al. 2013; Hassan et al. 2013 a, b; Gouda and El-Salakawy 2015; Hassan et al. 2017), there is a distinct lack of research on edge slab–column connections. Most of the existing studies have been focused on the behavior of two-way slabs reinforced solely with GFRP bars as flexural reinforcement. There is also the potential for FRP-shear reinforcement in the form of stirrups, shear studs, or shear bands to improve the punching-shear strength of two-way slabs reinforced with GFRP bars (Hassan et al. 2014 a, b; Gouda and El-Salakawy 2016; El-Gendy and El-Salakawy 2016; Mostafa and El-Salakawy 2018).

Based on these earlier studies, FRP shear reinforcement has demonstrated its ability to develop substantial increases in punching-shear and deformation capacities, making it an attractive alternative to traditional methods, such as drop panels and column capitals, for the construction of two-way GFRPRC slabs, especially when there are constraints on slab thickness. It is worth mentioning that the current North American codes for FRP—ACI 440.1R (2015) and CSA S806 (2012)—do not have provisions for designing GFRP-reinforced connections with FRP shear reinforcement. This is mainly due to a lack of experimental research, particularly on edge connections. Given the increase use of FRP as flexural and transverse shear reinforcement in different structural elements such as beams, beam–column joints, and piles, similar code provisions are urgently needed for two-way flat-slab structures reinforced with FRP flexural and shear reinforcement.

The experimental program presented herein is a part of an extensive research project at the Department of Civil Engineering at University of Sherbrooke with the aim of investigating the influence of GFRP-closed stirrups (closed and spiral) and extension inside the slab around the column perimeter on the punching-shear strength and failure within or outside the shear-reinforced zone. However, this paper presents preliminary results on the effects of GFRP closed stirrups as shear reinforcement on the punching-shear behavior of GFRP edge flat plate connections reinforced.

## 2 Experimental Program

### 2.1 Test Specimens

Three full-scale edge slab column connection specimens were constructed and tested to failure under combined vertical load and unbalanced moment. The slabs had identical geometries of 2500 × 1350 × 200 mm with a 300-mm square column stub protruding 700 mm above and below the slab surfaces. Table 1 presents the characteristics for only one specimen with typical details. The specimens were reinforced in the short and long directions, respectively, with 10 and 20 No. 20 bars as a flexural tension reinforcement in the bottom side and 7 and 10 No. 15 bars in the compression (top) side. The average bottom reinforcement ratio ($\rho_b$) was 1.55%, while the average compression (top) reinforcement ($\rho_t$) was 0.68%. The connections were reinforced in shear with four branches of No. 10 discrete closed or rectilinear spiral GFRP stirrups. The shear-reinforcement stirrups were arranged in a cruciform pattern according to ACI 318 (2014) and CSA A23.3 (2014). The number of peripheral lines of shear reinforcement was different according to the studied parameters; the spacing between the consecutive lines was 0.5d. The first perimeter was offset d/4 from the column face for all slabs with shear reinforcement, as specified in CSA A23.3 (2014). The shear-reinforcement ratio ($\rho_{fv}$) at the perimeter of 0.5d from the column face was maintained constant at 0.9%. Each slab was monolithic with a square column stub, which was designed to transfer shear force and lateral moment to the slab without any premature column failure. The column reinforcement consisted of six 25M deformed steel bars with 10M deformed closed steel ties at 100 mm. Figure 1 shows the typical flexural reinforcement details as well as shear reinforcement configurations of specimen G-CS-1.75d.

Table 1: Specimen details

| Test Specimen | $f_c'$, (MPa) | Average Flexural-Reinforcement Ratio | | Stirrup Layout Parameters | | | | |
|---|---|---|---|---|---|---|---|---|
| | | Bottom $\rho_b$, (%) | Top $\rho_t$, (%) | Shape | Diameter, (mm) | $S_o$; (mm) | $S_{fv}$; (mm) | Extent |
| G-CS-1.75d | 47.6 | 1.55 | 0.65 | Closed | 9.5 | 0.25d | 0.5d | 1.75d |

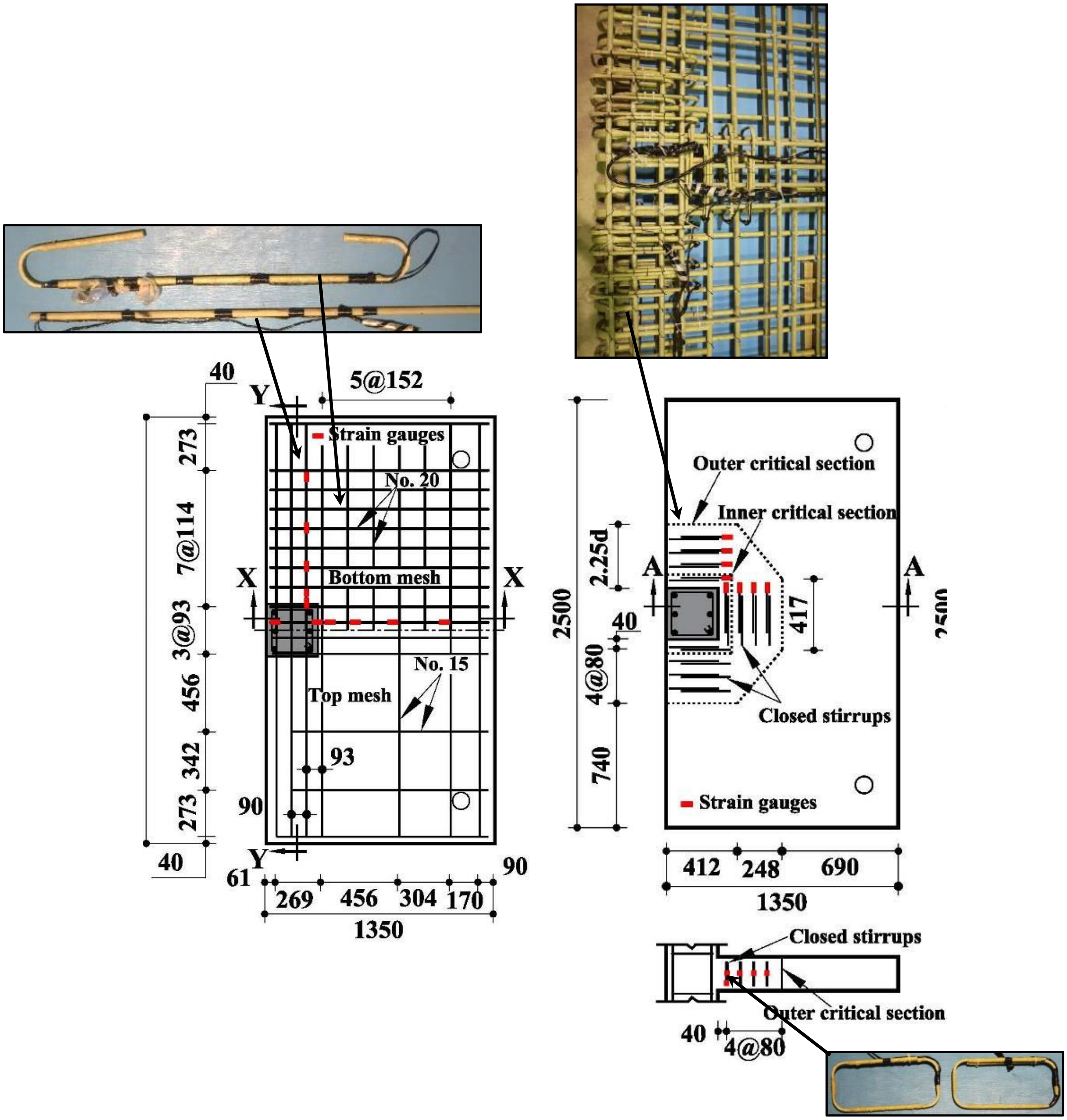


Figure 1: Details of test specimen: geometry, shear reinforcement configuration, and instrumentations (Note: All dimensions in mm)

## 2.2 Material Properties

Grade II and III sand-coated GFRP bars as classified in CSA S807 (2015) as No. 15 and No. 20 were used as flexural reinforcement. The specimens were reinforced with layers of straight GFRP bars, except for the tension reinforcement (bottom) in the long direction, which had double bent ends. That was to provide the required anchorage and avoid any unexpected mode of failure, such as slippage failure rather than punching failure. The tensile properties of the GFRP bars were determined by testing five representative specimens in accordance with ASTM D7205M (2011). Discrete No. 10 closed and rectilinear sand-coated spiral GFRP stirrups [290 mm wide × 145 mm high] were used as shear reinforcement. The tensile strengths of the straight and bent portions of the stirrups were determined by testing five representative specimens according to ASTM D7205M (2011) and the B.5 test method in ACI 440.3R (2004), respectively. Table 2 presents the tensile properties of the GFRP bars and stirrups. The specimens were cast using a ready-mixed, normal-weight concrete with a 28-day target concrete compressive strength of 35 MPa and 5 to 8% of entrained air. The concrete compressive ($f_c'$) was determined on the day of testing using at least three concrete cylinders measuring 100 mm × 200 mm for compression test as listed in Table 1.

Table 2. Tensile properties of the GFRP flexural bars and shear reinforcement

| Bar Designation[a] | Nominal cross-sectional area ($mm^2$) | Ultimate tensile strength (MPa) | Elastic tensile modulus (GPa) | Ultimate tensile strain (%) |
|---|---|---|---|---|
| **GFRP straight flexural bars** | | | | |
| No. 15 GFRP bar | 199 | 1323 ±12 | 64.8±0.5 | 2.2 ±0.05 |
| No. 20 GFRP bar | 285 | 1334 ±85 | 64.9±0.6 | 2.1 ±0.13 |
| **GFRP bent flexural bars** | | | | |
| No. 20 straight portion | 285 | 1210±63 | 53±0.48 | 2.3±0.15 |
| No. 20 bent portion | | $f_{fvb}$ [b]= 490±44 | ------ | ------ |
| **GFRP-stirrup shear reinforcement** | | | | |
| No. 10 straight portion | 71 | 967±39 | 45.7±0.5 | 2.1±0.08 |
| No. 10 bent portion | | $f_{fvb}$ [b]= 489±38 | ------ | ------ |

## 2.3 Instrumentations

Strains in the bottom flexural reinforcement (tension side) were measured with 11 electrical resistance strain gauges at different locations in both orthogonal directions. In addition, one electrical strain gauge was glued at the bend location of the GFRP bar at the column location. The strains in the FRP stirrups were monitored using six strain gauges mounted at mid-height of the vertical legs of the FRP stirrups and bend location in each orthogonal direction, as shown in Fig. 1. In addition, five concrete electrical strain gauges were glued before testing to the slab's top surface (compression side) at 0 and 200 mm from the column face. Sixteen string potentiometers (pots) were used at different locations to measure the displacements. During the test, crack propagation was marked, and the corresponding loads were recorded.

## 2.4 Test setup

The specimens were tested in the structural laboratory at the University of Sherbrooke until failure. The details of the test setup are shown in Fig. 2. Vertical shear force was simulated by vertically applying a downward load through the column using a 1500-kN hydraulic jack which was installed in the middle of a rigid steel I-beam supported on two steel portal frames. To facilitate a free horizontal movement of the column during lateral loading, a steel pan with rollers was placed between the vertical jack and the top of the upper concrete column. Two 1000-kN horizontal hydraulic jacks were installed on two very rigid reaction frames fixed firmly to the laboratory strong floor to apply lateral loads. The vertical and lateral jacks were controlled using three manual hydraulic pumps. The loads were monitored with three load cells on each pump and connected to the data-acquisition system. The specimen was simply supported on the bottom surface along three sides during testing with the fabricated supporting steel bed. The bottom supporting frame was braced with eight double angles back to back and pre-stressed to the laboratory floor with four 38 mm diameter steel tie rods to avoid any lateral movements. On the slab top face, three supported edges were restrained by steel reaction beams to prevent slab lifting. To simulate slab rotation at the lines of contra flexure during the entire test, neoprene bearing pads measuring 20 mm thick and 100 mm wide were placed between the slab and supporting bed and between the slab and top restrain beams along the support lines. The specimens were tested under unbalanced moment (Mun) to vertical load (V) ratio of 0.3 m. The unbalanced moments were calculated by multiplying the two lateral forces, applied to each column by the distance from the application point to the center of the slab: 675 mm. The vertical load was applied monotonically at a load-controlled rate of 5 kN/min, whereas the horizontal forces were simultaneously applied with the vertical force in small increments to maintain a constant moment-to-shear ratio of 0.3 m throughout the test until failure.

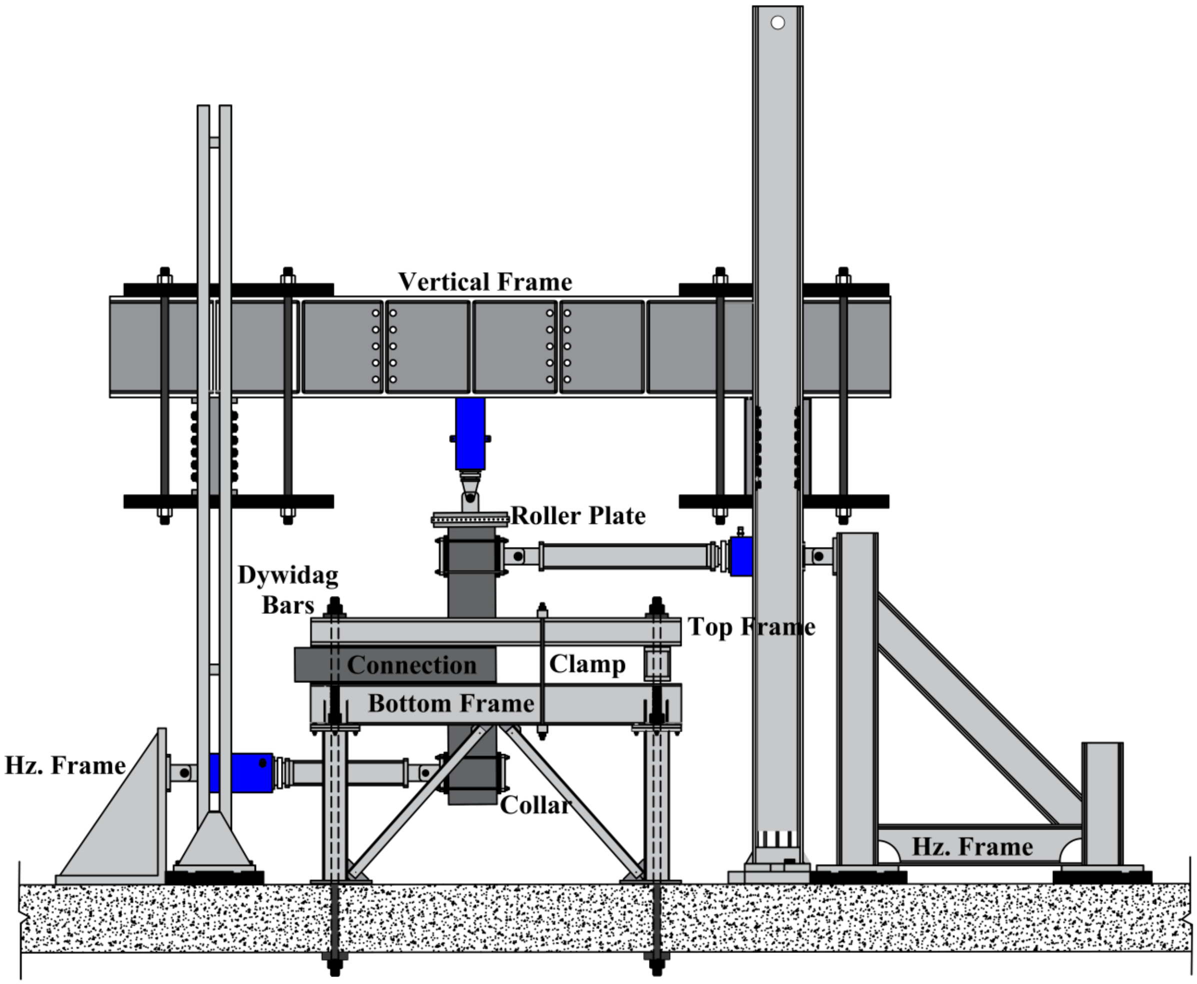


Figure 2: Test setup

## 3 Test Results and Discussions

The test results revealed that the presence of GFRP shear reinforcement as either closed or spiral stirrups within the slab around the column perimeter improved the punching-shear response of the tested connections. This behavior, however, was strongly influenced by the characteristics of the shear-reinforcement type and extension from the column faces. In the following sections, the test results of the specimen G-CS-1.75d, with stirrups extended 1.75d, are presented.

### 3.2 Crack Pattern and Failure Mode

Figure 3 shows the cracking patterns for G-CS-1.75d in tension and compression and along the free-edge sides. During the test, flexural cracks appeared first in the slab tension side. The first flexural crack began to appear at vertical load of 53 kN. These radial flexural cracks were originated from the inner slab–column interface and propagated towards the supports. Inclined torsion cracks were formed at the inner corners of the columns at about 35° from the slab edge. These cracks started to appear at about 25 % of the ultimate loads then propagated upward the slab edge to half of the slab depth at approximately 50% of the ultimate loads. Thereafter, circumferential (tangential) cracks were generated around the column and crossed over the radial cracks at higher loads while the torsion cracks continued their way to the compression face of the slab. As the loads increased, the number of such cracks and their widths in the column vicinity increased. Shear cracks initiated from the slab tension side and propagated towards the compression side of the slab until the failure occurred. The FRP stirrups effectively contributed in distributing the shearing forces to the uncracked concrete outside the shear-reinforced zone. The final mode of failure was sudden with higher deformations before failure. The slab free edge evidenced horizontal splitting cracks over the top of the shear stirrups near the column top before joining with inclined cracks that developed outside of the shear-reinforced zone. The angle of the shear crack at the free edge was 25º with respect to the slab tension side.

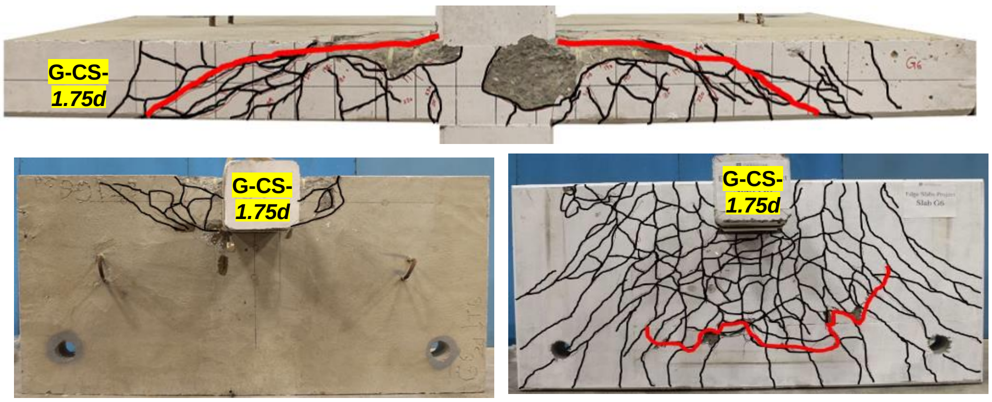


Figure 3: Cracking patterns and punching-shear failure surface (in bold)

### 3.3 Vertical Load-Deflection

Figure 4 plots the applied vertical load versus deflection relationships at 80 mm from the column face along the moment direction. Table 3 provides the maximum applied vertical load ($V_u$) and corresponding ultimate deflection ($\Delta_{Vu}$). The specimen G-CS-1.75d, including limited stirrups around the column produced bilinear load–deflection responses until the punching failure occurred abruptly, as shown in Fig. 4. G-CS-1.75d failed at 370 kN as an ultimate load and at 28 mm, corresponding to ultimate deflections along the moment direction.

Table 3: Test Results

| Test Specimen | Ultimate Load | | Deflection | Strains at Ultimate Load (µs) | | |
|---|---|---|---|---|---|---|
| | $V_u$, (kN) | $M_u$, (kN.m) | $\Delta_{vu}$, (mm) | Concrete | Flexural reinforcement | FRP stirrups @ 0.25 d |
| G-CS-1.75d | 370 | 115 | 28.08 | 979 | 8661 | 3918 |

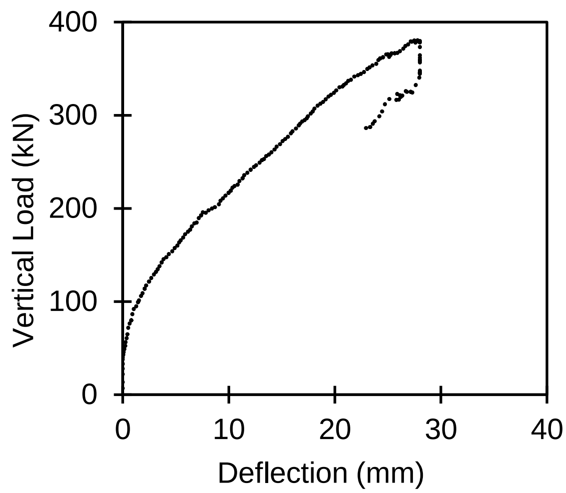


Figure 4: Load deflection relationship

### 3.4 Flexural and Shear Reinforcement Strains

Figure 5 plots the applied vertical load versus the flexural tension reinforcement strain. Table 3 reports the maximum reinforcement strain. Specimen G-CS-1.75d with shear reinforcement, exhibited higher strains in the GFRP reinforcing bars and lower concrete strains. This observation confirmed with previous findings for GFRP-reinforced interior slab–column connections with FRP stirrups (Hassan et. al 2014). The maximum reinforcement strain was 8661, representing 47% of the ultimate tensile strength. The maximum recorded concrete strain around the column was 979 which is low and below the concrete crushing strain of 3500 and 3000 μs, as per CSA S806 (2012) and ACI 440.1R (2015), respectively. The mode of failure of specimen G-CS-1.75d was triggered by brittle punching-shear failure occurring outside the shear-reinforced zone with no signs of concrete crushing in the compression zone or GFRP-bar rupture.

Figure 6 shows the measured strain at mid-height of the vertical legs of the FRP stirrups located at 0.25d, where d is the slab effective depth. As evidenced in Fig. 6, the contribution of the FRP stirrups to the punching-shear strength before cracking was insignificant. After the development of inclined shear cracks, however, the shear reinforcement transferred most of the forces across the shear cracks and delayed further widening. This, in turn, increased the punching-shear strength and deformation capacity of the test specimens (Rizk et al. 2011; Hassan et al. 2014).

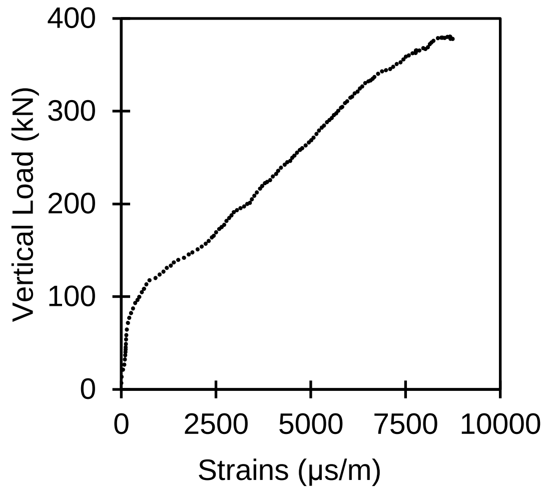

Figure 5: Load flexural strain relationship

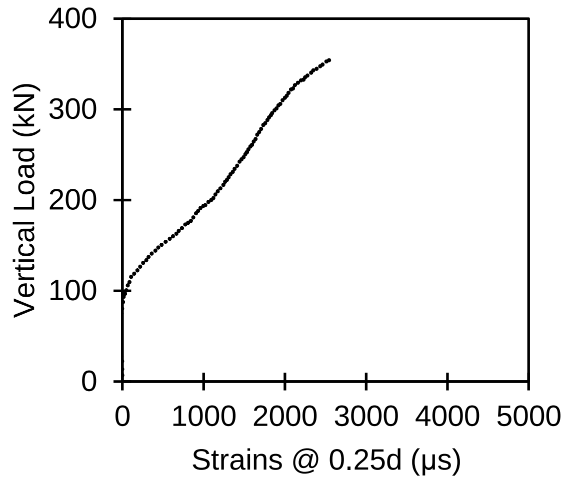

Figure 6: Load shear strain relationship

## 4 Conclusions

Based on the experimental results and discussions presented herein, the following conclusions are drawn:

1. Using closed stirrups as shear reinforcement offered sufficient resistance and confinement to control the development of large shear cracks and effectively distributed the shearing forces around the punching-shear zone.

2. The presence of shear reinforcement in the two-way flat slabs can transform the punching-shear failure into a ductile rather than brittle mode assuming no rupture of stirrups occurs.

3. This preliminary study confirms the efficiency of the FRP closed in increasing the punching-shear capacity as well as the deformation capacity. More investigations, however, are needed to examine the effect of GFRP shear reinforcement with different extensions around the column zone to quantify the concrete-fraction contribution outside the shear-reinforced zone and determinate the minimum extension limit of GFRP stirrups.

## 5 Acknowledgements


The authors wish to acknowledge the financial support of the Tier 1 Canada Research Chair in Advanced Composite Materials for Civil Structures, Natural Sciences and Engineering Research Council of Canada (NSERC Industrial Research Chair in Innovative FRP Reinforcement for Sustainable Concrete Infrastructure), the Canadian Foundation for Innovation (CFI), and the Fonds de recherché du Québec – Nature et Technologies – (FRQ-NT). The assistance of the technical staff of the Structural and Materials Laboratory in the Department of Civil Engineering at the University of Sherbrooke is also greatly appreciated


## 6 Notations

The following symbols are used in this paper

| | | |
|---|---|---|
| $d$ | = | effective slab depth |
| $d_b$ | = | bar diameter |
| $f_c'$ | = | concrete-cylinder compressive strength |
| $M_u$ | = | ultimate unbalanced moment at column centroid |

$s_{fv}$ = stirrup spacing

$V_u$ = ultimate vertical shear force at column centroid

$V_u$ = ultimate punching-shear load

$\Delta_{Vu}$ = ultimate deflection at peak load

$\varepsilon_{fv}$ = limiting tensile strain in FRP stirrups

$A_{fv}$ = cross-sectional area of the FRP shear reinforcement at a perimeter of 0.5*d* from column face

$\rho_b$ = average bottom flexural-reinforcement ratio

$\rho_t$ = average top flexural-reinforcement ratio

$\rho_{fv}$ = shear-reinforcement ratio at a perimeter of 0.5*d* from column face = ($n_s*A_{fv}/S_{fv}\,b_o$)

## 7 References


ACI Committee 440 2004. Guide test methods for fiber-reinforced polymers (FRPs) for reinforcing or strengthening concrete structures, Farmington Hills, MI, USA: American Concrete Institute, 2015, p. 40.

ACI Committee 440 2015. Guide for the Design and Construction of Concrete Reinforced with FRP Bars. (ACI 440.1R-2015). ACI, Farmington Hills, MI.

ASTM. 2011. Standard test method for tensile properties of fiber reinforced polymer matrix composite bars. ASTM D7205, West Conshohocken, PA.

Canadian Standards Association CSA 2012. Design and Construction of Building Structures with Fiber Reinforced Polymers. S806, CSA, Rexdale, Ontario, Canada.

Canadian Standards Association CSA 2014. Design of concrete structures for buildings. A23.3, CSA Rexdale, Ontario, Canada.

Canadian Standards Association CSA 2015. Specification for Fiber-Reinforced Polymers. S807, CSA, Rexdale, Ontario, Canada, 27 p.

Dulude, C., Hassan, M., Ahmed, E.A., and Benmokrane, B. 2013. Punching Shear Behaviour of Two-Way Flat Concrete Slabs Reinforced with GFRP Bars. ACI Structural Journal, 110(5): 723–734.

El-Gendy, M.; and El-Salakawy, E. 2015. Effect of Shear Studs and High Moments on Punching Behavior of GFRP-RC Slab–Column Edge Connections. Journal of Composites for Construction, DOI: 10.1061/(ASCE)CC.1943-5614.0000668

Gouda, A., and El-Salakawy, E. 2015. Punching Shear Strength of GFRP-RC Interior Slab-Column Connections Subjected to Moment Transfer. Journal of Composites for Construction, ASCE, V. 20, No. 1, Feb.

Gouda, A., and El-Salakawy, E. 2016. Behavior of GFRP-RC Interior Slab-Column Connections with Shear Studs and High-Moment Transfer. Journal of Composites for Construction, ASCE, V. 20, No. 4, Aug., doi: 10.1061/(ASCE)CC.1943-5614.0000663.10.1061/(ASCE)CC.1943-5614.0000663

Hassan M., Ahmed, E. A., and Benmokrane, B. 2013a. Punching- Shear Strength of GFRP-Reinforced Concrete Flat Slabs. Canadian Journal of Civil Engineering, V. 40, No. 10, Apr., pp. 951-960.

Hassan, M., Ahmed, E. A., and Benmokrane, B. 2013b. Punching-Shear Strength of Normal- and High-Strength Two-Way Concrete Slabs Reinforced with GFRP Bars. Journal of Composites for Construction, ASCE, V. 17, No. 6, Dec., doi: 10.1061/(ASCE)CC.1943-5614.0000424.10.1061/(ASCE)

Hassan, M., Ahmed, E. and Benmokrane, B. 2014a. Punching Shear Behavior of Two-Way Slabs Reinforced with FRP Shear Reinforcement. Journal of Composites for Construction, ASCE, V. 19, No.1, Feb., doi: 10.1061/(ASCE)CC.1943-5614.0000493.10.1061/(ASCE)

Hassan, M.; Ahmed, E.; and Benmokrane, B. 2014b. Punching-Shear Design Equation for Two-Way Concrete Slabs Reinforced with FRP Bars and Stirrups. Construction and Building Materials, V. 66, Sept., pp. 522-532.

Hassan, M.; Fam, A., Benmokrane, B., and Ferrier, E. 2017. Effect of Column Size and Reinforcement Ratio on Shear Strength of Glass Fiber-Reinforced Polymer Reinforced Concrete Two-Way Slabs. ACI Structural Journal, V. 114, No. 4, July-August.

Lee, J.H., Yoon, Y.S., and Mitchell, D. 2009. Improving Punching Shear Behavior of Glass Fiber-Reinforced Polymer Reinforced Slabs. ACI Structural Journal, 106(4): 427–434.

Lips, S.; Ruiz, M.; and Muttoni A. 2012. Experimental Investigation on Punching Strength and Deformation Capacity of Shear-Reinforced Slabs. ACI Structural Journal, V. 109, No. 6, Nov.-Dec., pp. 889-900.

Megally, S., and Ghali, A. 2000. Seismic Behavior of Slab-Column Connections. Canadian Journal of Civil Engineering, V. 27, No. 1, pp. 84-100.

Mostafa, A., and El-Salakawy, E. 2018 "Behavior of GFRP-RC Slab–Column Edge Connections with High-Strength Concrete and Shear Reinforcement," Journal of Composites for Construction, DOI: 10.1061/(ASCE)CC.1943-5614.0000831.

Ospina, C.E., Alexander, S.D. B., and Roger Cheng, J.J. 2003 "Punching of Two-Way Concrete Slabs with Fiber-Reinforced Polymer Reinforcing Bars or Grids." ACI Structural Journal, 100(5): 589–598.

Rizk, E., Marzouk, H., Hussein, A, (2011), Punching Shear of Thick Plates with and Without Shear Reinforcement. ACI Structural Journal, 108 (5): 581-591.